CAMBRIDGE
UNIVERSITY PRESS

RESEARCH ARTICLE

Symbolic position analysis for three 6-DOF parallel mechanisms and new insight

Zhongqiu Du, Ju Li, Qingmei Meng, Pengda Ye and Huiping Shen

Research Center for Advanced Mechanisms Theory, Changzhou University, Changzhou, PR China
Corresponding author: Huiping Shen; Email: shp65@126.com

Abstract

The authors' previous research has demonstrated that parallel mechanisms (PMs) with hybrid branch chains (i.e., branch chains containing planar or spatial loops) can possess symbolic forward position (SFP) solutions and motion decoupling (MD). In order to further study the conditions of a three-chain six degrees of freedom (DOF) parallel mechanism with SFP and MD, this paper proposes one 6-DOF branch chain A and two 5-DOF branch chains B and C. Based on these, a class of four 6-DOF PMs with three branch chains is devised. The symbolic position analysis of three of four such PMs is performed consequently, featuring partial MD and SFPs, which reveals that if the position or orientation of a point on the moving platform can be determined by the position of the hybrid branch chain, the PM exhibits partial MD and SFP. Finally, the accuracy of the symbolized forward and inverse solution algorithms is verified through numerical examples. This research brings a new insight into the design and position analysis of 6-DOF PMs, particularly those with SFP and partial MD.

1. Introduction

Generally, as the number of parallel branch chains increases in a parallel mechanism (PM), the workspace-to-volume ratio decreases and flexibility decreases, increasing the likelihood of interference. Additionally, there are more singular configurations, and the kinematic solutions become more complex [1]. Therefore, for a 6-DOF PM with a complex topology and strong loop coupling, reducing the number of branch chains and cleverly designing the topology can effectively address these drawbacks.

Consequently, a minimally-constrained 6-DOF PM proves to be a viable solution. Some progress has been made in researching 6-DOF PMs with three limbs such as 3-PPSP, 3-RRPS, 3-PRPS, and 3-URS. However, these minimally-constrained 6-DOF PMs still exhibit limitations such as non-decoupled motion and complex forward kinematics.

Currently, there are very few 6-DOF PMs with decoupled position and motion, as well as symbolic forward and inverse kinematics. Nevertheless, a 6-DOF 6-SPU PM with a spherical joint, double spherical joint, and triple spherical joint (1-2-3 type) on the moving platform does possess symbolic forward and inverse kinematics, as well as decoupled position and orientation [2]. Consequently, subsequent kinematic studies, dynamic analysis, and control research of this mechanism are facilitated [3].

The position analysis of 6-DOF PMs, which is a critical issue in kinematic problems, has been extensively studied by many researchers. There are two main methods commonly adopted algebraic analytical methods and numerical methods [3, 4]. The author has recently proposed a distinction between analytical solutions, categorizing them as either symbolic solutions or closed-form solutions (in the form of a univariate polynomial equation). These two types of solutions differ in their mathematical representation: symbolic solutions can be expressed as formulaic expressions, while closed-form solutions can only be represented as univariate polynomial equations, and the final solution is in numerical form. This differentiation provides a clear and distinct categorization [3].

Algebraic methods are widely used for the analysis of 6-DOF PMs, particularly for 6-SPS PMs and their derived types. Among them, Innocenti *et al.* [5] solved the closed-form solution of the 5-5 type PM. Lin *et al.* [6] conducted a forward position analysis of the 4-5 type PM and obtained closed-form solutions. Huang *et al.* [7] utilized algebraic algorithms to solve the forward kinematics of a 6-6 type PM, resulting in a high-order equation of degree 40 in one variable. Lin [8] and others derived 20 input-output equations for the 6-5 platform spatial PM and obtained 40 different poses for the moving platform. Zhang *et al.* [9] proposed an algebraic elimination method to solve the forward kinematics of the general 6-4 PM and obtained a high-order equation of degree 1 for its forward kinematics. Su *et al.* [10] applied Dixon's resultant to analyze the forward kinematics of a 5-5 PM, resulting in its input-output equation of degree 40 in one variable and all the solutions. Yun *et al.* [11] designed a three-legged 6-DOF PM and analyzed its forward and inverse kinematics. Gao [12, 13] studied the closed-form solutions of the forward and inverse kinematics of the 6-DOF 2-SRU mechanism and 3-UPS mechanism, respectively. Yu *et al.* [14] analyzed the position of the 6-DOF 3-UrSR PM and obtained the closed-form solution of its forward kinematics.

On the other hand, scholars who employ numerical methods include Innocenti *et al.* [15], Dasgupta *et al.* [16], Husty *et al.* [17], Wampler *et al.* [18], Nanua *et al.* [19], and Lin *et al.* [20], who conducted research on the kinematic position analysis of 6-SPS PMs and their derived types. He *et al.* [21, 22] utilized a hybrid algorithm based on genetic algorithms and neural networks to analyze the forward kinematics of a 6-DOF PM with a 5R closed-loop five-bar linkage structure. Zhao *et al.* [23] used the direction cosine matrix method to solve the forward and inverse kinematics of the proposed orthogonal 6-DOF 6-PPPS PM. Shen *et al.* [24] proposed a new type of 6-DOF PM and proposed a numerical method for solving the forward kinematics of 6-SPS PMs based on a topological structure analysis in ref. [2], and in ref. [25], they suggested a 1-2-3-SPS PM and obtained its symbolic solutions. Wang *et al.* [26] proposed a mixed strategy combining a linear decoupling geometric analysis method and a high-order convergence iteration method to solve the forward kinematics of PMs. Chen *et al.* [27] proposed a 6-DOF PM with a branched closed-loop dual-drive unit capable of achieving hybrid output and conducted kinematic studies on it. Qu *et al.* [28] conducted a kinematic analysis of the 6-SPS parallel robot based on the differential evolution algorithm.

In Ref. [29], a three-branch 6-DOF PM is proposed and its kinematic position is analyzed. The numerical solution of the forward kinematics of the PM is obtained by Newton iteration method, and the symbolic forward position solution of the PM is derived. As we all know, it has the characteristics of symbolic forward position (SFP), which brings a lot of convenience for the subsequent error analysis, dynamic analysis, and real-time motion control of PM. In order to further study the conditions of a three-chain 6-DOF parallel mechanism with SFP and MD. Therefore, this paper proposes a class of four three-chain 6-DOF PMs, consisting of a designed 6-DOF chain A and 5-DOF chain C. Three of four PMs are revealed to exhibit SFP and partial DM. Furthermore, SFP and inverse solutions are derived for the three 6-DOF PMs. Numerical validations of the symbolic position solutions are also performed.

The work reveals a new rule, i.e., if the position or orientation of a point on the moving platform can be determined by the position of its one branch chain, the PM exhibits partial MD and SFP, which is a new insight for the design and position analysis of 6-DOF PMs, particularly for those with SFP and partial MD.

2. Design of a 6-DOF chain A and two 5-DOF chains B and C

According to the topological design theory of serial mechanism based on the position and orientation characteristics (POC) equation [3, 30], the following hybrid chains containing a 2-DOF planar five-bar mechanism (i.e., hybrid chain A, B) or a 1-DOF planar four-bar mechanism (i.e., hybrid chain C) are proposed.

For hybrid chain A, it consists of a 2-DOF planar five-bar mechanism connected in series with a 1-DOF rotating joint (R) and a 3-DOF spherical joint (S), resulting in a total of 6-DOF, as shown in Fig. 1(a).

Table I. *Types of parallel mechanisms.*

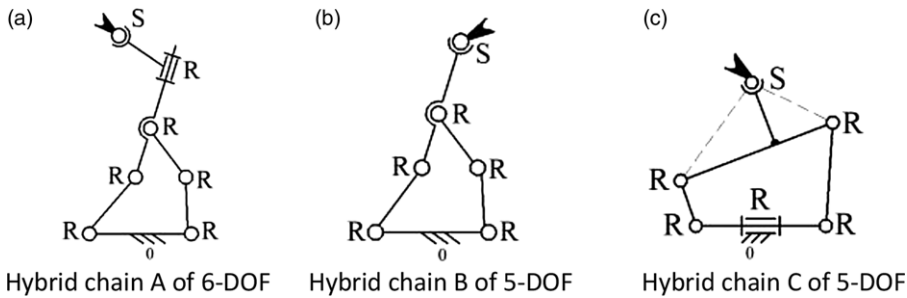| POC	0T3R	1T3R	2T3R	3T3R
			2A1B	3A
		1A2B		
Configuration of mechanism	3B		1A1B1C	2A1C
				3C
		1C2B	1B2C	
				1A2C

Figure 1. *Hybrid branch chains A of 6-DOF, B and C of 5-DOF.*

For hybrid chain B, it directly connects a 2-DOF planar five-bar mechanism with a 3-DOF spherical joint (S), resulting in a total of 5-DOFs, as shown in Fig. 1(b).

Here, "2-DOF planar five-bar mechanism" refers to a planar mechanism composed of five rotating joints and five components. It has 2 degrees of freedom.

For hybrid chain C, it combines the base link of a 1-DOF planar four-bar mechanism with a 1-DOF rotating joint (R) and further connects it with a 3-DOF spherical joint (S) on its link, resulting in a total of 5-DOF, as shown in Fig. 1(c).

According to the topological design theory of PM based on the POC [30], the following three branched-chain mechanisms can be constructed from the above three hybrid branched-chain mechanisms, as shown in Table I. There are four three-branched 6-DOF mechanisms, respectively, referred to as 3A, 3C, 1A + 2C, and 2A + 1C mechanisms, as shown in Fig. 2.

The position analysis of PM1 has been conducted in Ref. [29], which indicates that this PM exhibits non-MD and lacks SFPs.

However, the work of the paper reveals that the proposed PM2, PM3, and PM4 possess SFP solutions and partially MD. Thus, in this paper, the position analysis of these three 6-DOF PMs is carried out, shedding light on the paradigm for solving the position equations of such three-chain 6-DOF PMs.

3. Kinematic position analysis of PMs

3.1. Position analysis of the PM2

The coordinate system established by PM2 is illustrated in Fig 3(a). The base coordinate system is established at one corner of a regular cube with edge length 2a. The X, Y, and Z axes are perpendicular and orthogonal to each other. Each hybrid branch chain is located at the geometric center of one of the three orthogonal faces of the cube. Moreover, the X-axis is perpendicular to the line $A_{12}A_{22}$, the Y-axis is perpendicular to the line $A_{32}A_{41}$, and the Z-axis is perpendicular to the line $A_{52}A_{61}$. The moving coordinate system is established at the geometric center of the moving platform (an equilateral triangle). The x-axis points toward S_1, the y-axis is parallel to the line S_2S_3, and the z-axis is determined by the right-hand screw rule.
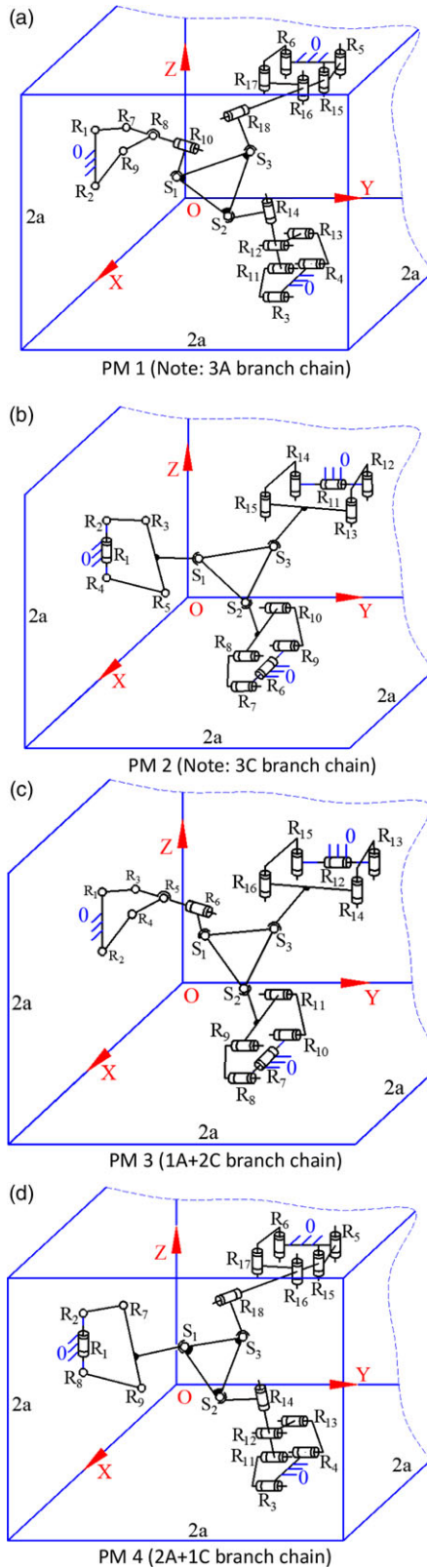
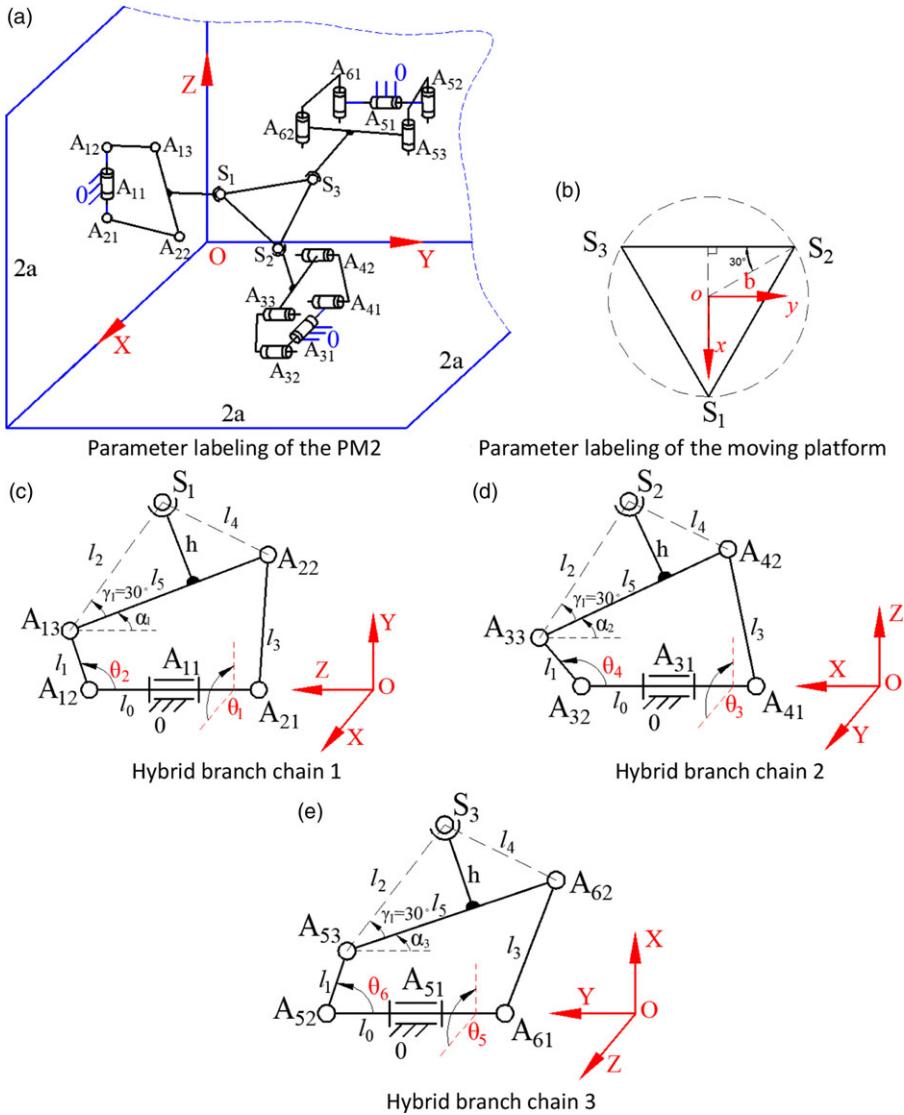**Figure 2.** *A class of four 6-DOF parallel mechanisms.*

Figure 3. *Kinematic parameters labeling of parallel mechanism 2.*

The distance from the geometric center of the movable platform to each vertex of the equilateral triangle is denoted as b, as shown in Fig 3(b). The parameters of each hybrid branch are labeled as shown in Figs 3(c-e), and the rod length parameters are as follows:

$A_{11}A_{12} = A_{11}A_{21} = A_{31}A_{32} = A_{31}A_{41} = A_{51}A_{52} = A_{51}A_{61} = l_0$, $A_{12}A_{13} = A_{32}A_{33} = A_{52}A_{53} = l_1$, $A_{13}S_1 = A_{33}$ $S_2 = A_{53}S_3 = l_2$, $A_{21}A_{22} = A_{41}A_{42} = A_{61}A_{62} = l_3$, $A_{22}S_1 = A_{42}S_2 = A_{62}S_3 = l_4$, $A_{13}A_{22} = A_{33}A_{42} = A_{53}A_{62} = l_5$. The distance between each spherical joint center and rod 5 is denoted as h.

3.1.1. Forward position analysis of the PM2

Given the input $\theta_i (i = 1 \sim 6)$ of the driving joints, to determine the posture of the moving platform.

Suppose the coordinates of any point S_i $(i = 1 \sim 3)$ on the moving platform in the moving coordinate system are denoted as S_i', and the origin O' of the moving coordinate system has coordinates S_o (x, y, z) in the base coordinate system. Then, the coordinates of any point S_i on the moving platform in the base coordinate system can be expressed as follows:

$$S_i = QS'_i + S_0 \tag{1}$$

Here, Q represents the transformation matrix from the moving coordinate system to the base coordinate system.

Due to the end POC of the moving platform being 3T3R, where α, β, and γ represent the rotating angles of the moving platform around the x, y, and z axes, respectively, Q can be expressed as:

$$Q = \begin{bmatrix} \cos \beta \cos \gamma & -\cos \beta \sin \gamma & \sin \beta \\ \sin\alpha \sin \beta \cos \gamma + \cos \alpha \sin \gamma & \cos \alpha \cos \gamma - \sin\alpha \sin \beta \sin \gamma & -\sin \alpha \cos \beta \\ \sin \alpha \sin \gamma - \cos\alpha \sin \beta \cos \gamma & \cos\alpha \sin \beta \sin \gamma + \sin \alpha \cos \gamma & \cos \alpha \cos \beta \end{bmatrix} \tag{2}$$

The coordinates of the vertices of the moving platform in the moving coordinate system are given as:

$$S'_1 = (b, 0, 0), S'_2 = \left(-b/2, \sqrt{3}b/2, 0\right), S'_3 = \left(-b/2, -\sqrt{3}b/2, 0\right).$$

According to Eq. (1), the coordinates of the three vertices $S_1 \sim S_3$ of the moving platform in the base coordinate system can be obtained as follows:

$$\begin{cases} x_{s1} = b \cos \beta \cos \gamma + x \\ y_{s1} = b (\sin\alpha \sin \beta \cos \gamma + \cos \alpha \sin \gamma) + y \\ z_{s1} = b (\sin \alpha \sin \gamma - \cos\alpha \sin \beta \cos \gamma) + z \end{cases} \tag{3}$$

$$\begin{cases} x_{s2} = -\dfrac{b}{2} \cos \beta \cos \gamma - \dfrac{\sqrt{3}}{2} b \cos \beta \sin \gamma + x \\ y_{s2} = -\dfrac{b}{2} (\sin\alpha \sin \beta \cos \gamma + \cos \alpha \sin \gamma) + \dfrac{\sqrt{3}b}{2} (\cos \alpha \cos \gamma - \sin\alpha \sin \beta \sin \gamma) + y \\ z_{s2} = -\dfrac{b}{2} (\sin \alpha \sin \gamma - \cos\alpha \sin \beta \cos \gamma) + \dfrac{\sqrt{3}b}{2} (\cos\alpha \sin \beta \sin \gamma + \sin \alpha \cos \gamma) + z \end{cases} \tag{4}$$

$$\begin{cases} x_{s3} = -\dfrac{b}{2} \cos \beta \cos \gamma + \dfrac{\sqrt{3}b}{2} \cos \beta \sin \gamma + x \\ y_{s3} = -\dfrac{b}{2} (\sin\alpha \sin \beta \cos \gamma + \cos \alpha \sin \gamma) - \dfrac{\sqrt{3}}{2} b (\cos \alpha \cos \gamma - \sin\alpha \sin \beta \sin \gamma) + y \\ z_{s3} = -\dfrac{b}{2} (\sin \alpha \sin \gamma - \cos\alpha \sin \beta \cos \gamma) - \dfrac{\sqrt{3}}{2} b (\cos\alpha \sin \beta \sin \gamma + \sin \alpha \cos \gamma) + z \end{cases} \tag{5}$$

1) Analysis of hybrid branch chain 1

For analysis of forward position for hybrid branch chain 1, the line $A_{13}S_1$ is perpendicular to the line $A_{22}S_1$ in hybrid branch chain 1, and the angle between the line $A_{13}S_1$ and $A_{13}A_{22}$ is $\gamma_1 = 30°$.

Furthermore, the angle between link $A_{13}A_{22}$ and the negative direction of the Z-axis is set as α_1 and used as an intermediate variable.

It's easy to know the coordinates of the following points.

$A_{11} = (a, 0, a), A_{21} = (a, 0, a - l_0), A_{12} = (a, 0, a + l_0), A_{13} = (a + l_1 \sin \theta_2 \cos \theta_1, l_1 \sin \theta_2 \sin \theta_1, a + l_0 - l_1 \cos \theta_2)$,

$A_{22} = (a + (l_1 \sin \theta_2 + l_5 \sin \alpha_1) \cos \theta_1, (l_1 \sin \theta_2 + l_5 \sin \alpha_1) \sin \theta_1, a + l_0 - l_1 \cos \theta_2 - l_5 \cos \alpha_1)$.

According to the link length equation by constraint $A_{21}A_{22} = l_3$, the intermediate variable α_1 is found as

$$\alpha_1 = 2 \arctan \left(\frac{N_1 + n\sqrt{N_1^2 + N_2^2 - N_3^2}}{N_2 + N_3} \right) (n = \pm 1) \tag{6}$$

Where: $N_1 = 2l_1 l_5 \sin \theta_2$, $N_2 = -2l_5(2l_0 - l_1 \cos \theta_2)$, $N_3 = l_3^2 - l_5^2 - (l_1 \sin \theta_2)^2 - (2l_0 - l_1 \cos \theta_2)^2$.

Then the coordinates of S_1 are expressed as

$$
\begin{cases}
x_{s1} = a + (l_1 \sin \theta_2 + l_2 \sin (\gamma_1 + \alpha_1)) \cos \theta_1 \\
y_{s1} = (l_1 \sin \theta_2 + l_2 \sin (\gamma_1 + \alpha_1)) \sin \theta_1 \\
z_{s1} = a + l_0 - l_1 \cos \theta_2 - l_2 \cos (\gamma_1 + \alpha_1)
\end{cases}
\tag{7}
$$

2) Analysis of hybrid branch chain 2

The angle between link $A_{33}A_{42}$ in hybrid branch chain 2 and the negative direction of the X-axis is defined as α_2, and serves as an intermediate variable. It is easy to know the following coordinates.

$A_{31} = (a, a, 0)$, $A_{32} = (a + l_0, a, 0)$, $A_{41} = (a - l_0, a, 0)$,

$A_{33} = (a + l_0 - l_1 \cos \theta_4, a + l_1 \sin \theta_4 \cos \theta_3, l_1 \sin \theta_4 \sin \theta_3)$,

$A_{42} = (a + l_0 - l_1 \cos \theta_4 - l_5 \cos \alpha_2, a + (l_1 \sin \theta_4 + l_5 \sin \alpha_2) \cos \theta_3, (l_1 \sin \theta_4 + l_5 \sin \alpha_2) \sin \theta_3)$.

Based on the link length equation by constraint $A_{41}A_{42} = l_3$, we get the intermediate variable α_2 below

$$
\alpha_2 = 2 \arctan \left(\frac{M_1 + m\sqrt{M_1^2 + M_2^2 - M_3^2}}{M_2 + M_3} \right) \quad (m = \pm 1)
\tag{8}
$$

Where: $M_1 = 2l_5 l_1 \sin \theta_4$, $M_2 = -2l_5(2l_0 - l_1 \cos \theta_4)$, $M_3 = l_3^2 - l_5^2 - (l_1 \sin \theta_4)^2 - (2l_0 - l_1 \cos \theta_4)^2$.

Then the coordinates of S_2 are expressed as

$$
\begin{cases}
x_{s2} = a + l_0 - l_1 \cos \theta_4 - l_2 \cos (\gamma_1 + \alpha_2) \\
y_{s2} = a + (l_1 \sin \theta_4 + l_2 \sin (\gamma_1 + \alpha_2)) \cos \theta_3 \\
z_{s2} = (l_1 \sin \theta_4 + l_2 \sin (\gamma_1 + \alpha_2)) \sin \theta_3
\end{cases}
\tag{9}
$$

3) Analysis of hybrid branch chain 3

Similarly, let the angle between the link $A_{53}A_{62}$ in hybrid branch chain 3 and the negative Y-axis be α_3, which serves as an intermediate variable. It is also easy to know the following coordinates.

$A_{51} = (0, a, a)$, $A_{52} = (0, a + l_0, a)$, $A_{61} = (0, a - l_0, a)$, $A_{53} = (l_1 \sin \theta_6 \sin \theta_5, a + l_0 - l_1 \cos \theta_6, a + l_1 \sin \theta_6 \cos \theta_5)$,

$A_{62} = ((l_1 \sin \theta_6 + l_5 \sin \alpha_3) \sin \theta_5, a + l_0 - l_1 \cos \theta_6 - l_5 \cos \alpha_3, a + (l_1 \sin \theta_6 + l_5 \sin \alpha_3) \cos \theta_5)$.

Based on the link length equation by constraint $A_{61}A_{62} = l_3$, the intermediate variable α_3 is given below

$$
\alpha_3 = 2 \arctan \left(\frac{Q_1 + q\sqrt{Q_1^2 + Q_2^2 - Q_3^2}}{Q_2 + Q_3} \right) \quad (q = \pm 1)
\tag{10}
$$

Where: $Q_1 = 2l_5 l_1 \sin \theta_6$, $Q_2 = -2l_5(2l_0 - l_1 \cos \theta_6)$, $Q_3 = l_3^2 - l_5^2 - (l_1 \sin \theta_6)^2 - (2l_0 - l_1 \cos \theta_6)^2$.

Then the coordinates of S_3 are expressed as

$$
\begin{cases}
x_{s3} = (l_1 \sin \theta_6 + l_2 \sin (\gamma_1 + \alpha_3)) \sin \theta_5 \\
y_{s3} = a + l_0 - l_1 \cos \theta_6 - l_2 \cos (\gamma_1 + \alpha_3) \\
z_{s3} = a + (l_1 \sin \theta_6 + l_2 \sin (\gamma_1 + \alpha_3)) \cos \theta_5
\end{cases}
\tag{11}
$$

To here, the coordinate values of S_1, S_2, and S_3 are determined. Therefore, according to Eqs. (3)-(5), it is easy to know that the expression of the posture parameters of the moving platform of the 6-DOF PM is given below.

$$
\begin{cases}
x = \dfrac{x_{s1} + x_{s2} + x_{s3}}{3} \\[2mm]
y = \dfrac{y_{s1} + y_{s2} + y_{s3}}{3} \\[2mm]
z = \dfrac{z_{s1} + z_{s2} + z_{s3}}{3} \\[2mm]
\gamma = \arctan\left[(x_{s3} - x_{s1}) / \left(\sqrt{3}\,(x_{s1} - x)\right) \right] \\[2mm]
\beta = \arccos\left[(x_{s1} - x) / (b\cos\gamma) \right] \\[2mm]
\alpha = \arctan\left[\dfrac{\sqrt{3}\,(y_{s1} - y)\cos\gamma - (y_{s2} - y_{s3})\sin\gamma}{\sqrt{3}\,(y_{s1} - y)\sin\gamma\sin\beta + (y_{s2} - y_{s3})\cos\gamma\sin\beta} \right]
\end{cases}
\tag{12}
$$

Obviously, from the forward position analysis of the PM2, it can be inferred that the coordinate values of points S_1, S_2, and S_3 on the moving platform of PM2 can be obtained by solving the hybrid branch chain to which it belongs. Therefore, when any one of the points S_1, S_2, and S_3 is taken as the base point, i.e., the origin of the moving coordinate system, the PM has partial motion decoupling.

3.1.2 Inverse position analysis of the PM2
Given the position and postures of the moving platform of the PM2, to get the driving input $\theta_i (i = 1 \sim 6)$.

1) Hybrid branch chain 1
   From Eq (7), it is easy to know the following formula.

$$
\theta_1 = \arctan\left(\frac{y_{s1}}{x_{s1} - a} \right)
\tag{13}
$$

$$
\theta_2 = 2\arctan\left(\frac{f_1 + F\sqrt{f_1^2 + f_2^2 - f_3^2}}{f_2 + f_3} \right) \quad (F = \pm 1)
\tag{14}
$$

Where: $f_1 = \frac{-2l_1 y_{s1}}{\sin\theta_1}, f_2 = 2l_1\,(z_{s1} - a - l_0), f_3 = l_2^2 - l_1^2 - (y_{s1}/\sin\theta_1)^2 - (z_{s1} - a + l_0)^2$.

2) Hybrid branch chain 2
   From Eq. (9), we have

$$
\theta_3 = \arctan\left(\frac{z_{s2}}{y_{s2} - a} \right)
\tag{15}
$$

$$
\theta_4 = 2\arctan\left(\frac{g_1 + G\sqrt{g_1^2 + g_2^2 - g_3^2}}{g_2 + g_3} \right) \quad (G = \pm 1)
\tag{16}
$$

Where: $g_1 = \frac{-2l_{11} z_{s2}}{\sin\theta_3}, g_2 = 2l_1\,(x_{s2} - a - l_0), g_3 = l_2^2 - l_1^2 - (z_{s2}/\sin\theta_3)^2 - (x_{s2} - a + l_0)^2$.

3) Hybrid branch chain 3
   From Eq. (11), we get

$$
\theta_5 = \arctan\left(\frac{x_{s3}}{z_{s3} - a} \right)
\tag{17}
$$

$$
\theta_6 = 2\arctan\left(\frac{k_1 + K\sqrt{k_1^2 + k_2^2 - k_3^2}}{k_2 + k_3} \right) \quad (K = \pm 1)
\tag{18}
$$

Where: $k_1 = \frac{-2l_1 x_{s3}}{\sin\theta_5}, k_2 = 2l_1\,(y_{s3} - a - l_0), f_3 = l_2^2 - l_1^2 - (x_{s3}/\sin\theta_5)^2 - (y_{s3} - a + l_0)^2$.
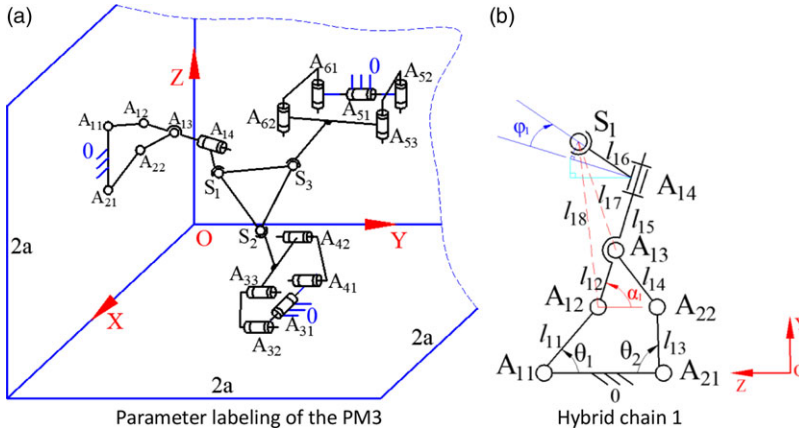
Figure 4. *Kinematic parameter labeling of the parallel mechanism 3.*

3.2. Position analysis of the PM3

The coordinate system established by PM3 is shown in Fig. 4(a). The base coordinate system is established at one corner of a regular cube with edge length of 2a, where the X-axis, Y-axis, and Z-axis are perpendicular and orthogonal. Each hybrid branch chain is located at the geometric center of one of the three orthogonal faces of the regular cube. In addition, the X-axis is perpendicular to the line $A_{11}A_{21}$, the Y-axis is perpendicular to the line $A_{32}A_{41}$, and the Z-axis is perpendicular to the line $A_{52}A_{61}$. The dynamic coordinate system is established at the geometric center of the moving platform (an equilateral triangle), where the x-axis points toward S_1, the y-axis is parallel to the line S_2S_3, and z-axis is determined by the right-hand screw rule.

The moving platform geometry and parameter annotation of PM3 are the same as those of PM2, as shown in Fig. 3(b). The parameter annotation of hybrid branch chain 1 is shown in Fig. 4(b), and the rod length parameters are as follows: $A_{11}A_{21} = l_{10}$, $A_{11}A_{12} = l_{11}$, $A_{12}A_{13} = l_{12}$, $A_{21}A_{22} = l_{13}$, $A_{22}A_{13} = l_{14}$, $A_{13}A_{14} = l_{15}$, $A_{14}S_1 = l_{16}$. The parameters of the other hybrid branch chains are the same as PM2.

3.2.1 Forward position analysis of the PM3

The angle between the link $A_{12}A_{13}$ and the positive direction of the Z-axis is denoted as α_1, and serves as an intermediate variable. It's easy to know the coordinates of the following points.

$A_{11} = (a, 0, a + l_{10}/2)$, $A_{21} = (a, 0, a - l_{10}/2)$, $A_{12} = (a, l_{11} \sin \theta_1, a + l_{10}/2 - l_{11} \cos \theta_1)$,

$A_{22} = (a, l_{13} \sin \theta_2, a - l_{10}/2 + l_{13} \cos \theta_2)$, $A_{13} = (a, l_{11} \sin \theta_1 + l_{12} \sin \alpha_1, a + l_{10}/2 - l_{11} \cos \theta_1 - l_{12} \cos \alpha_1)$,

$A_{14} = (a, l_{11} \sin \theta_1 + (l_{12} + l_{15}) \sin \alpha_1, a + l_{10}/2 - l_{11} \cos \theta_1 - (l_{12} + l_{15}) \cos \alpha_1)$.

According to the link length equation by constraint $A_{13}A_{22} = l_4$, the intermediate variable α_1 is obtained as

$$\alpha_1 = 2 \arctan \left(\frac{N_1 + n\sqrt{N_1^2 + N_2^2 - N_3^2}}{N_2 + N_3} \right) (n = \pm 1) \tag{19}$$

Where: $N_1 = 2l_{12}(l_{11} \sin \theta_1 - l_{13} \sin \theta_2)$, $N_2 = -2l_{12}(l_{10} - l_{11} \cos \theta_1 - l_{13} \cos \theta_2)$,

$N_3 = l_{14}^2 - l_{12}^2 - (l_{11} \sin \theta_1 - l_{13} \sin \theta_2)^2 - (l_{10} - l_{11} \cos \theta_1 - l_{13} \cos \theta_2)^2$.

Let the rotation angle of R_{10} from the YOZ plane be φ_1, as shown in Fig. 4(b). Then the coordinates of S_1 can be expressed as

$$\begin{cases} x_{s1} = x_{A14} - l_{16} \sin \varphi_1 \\ y_{s1} = y_{A14} + l_{16} \cos \varphi_1 \cos \alpha_1 \\ z_{s1} = z_{A14} + l_{16} \cos \varphi_1 \sin \alpha_1 \end{cases} \tag{20}$$

The angle φ_1 in the hybrid branch chain 1 can be obtained by the link length constraint $S_1S_2 = \sqrt{3}b$.

$$\varphi_1 = 2 \arctan \left(\frac{W_1 + w\sqrt{W_1^2 + W_2^2 - W_3^2}}{W_2 + W_3} \right) (w = \pm 1) \tag{21}$$

Where, $W_1 = -2l_{16} \cos \alpha_1 (x_{A14} - x_{s2})$, $W_2 = 2l_{16}(y_{A14} - y_{s2}) \cos \alpha_1 + 2l_{16}(z_{A14} - z_{s2}) \sin \alpha_1$, $W_3 = 3b^2 - l_{16}^2 - (x_{s2} - x_{A14})^2 - (y_{s2} - y_{A14})^2 - (z_{s2} - z_{A14})^2$.

The hybrid branch chains 2 and 3 in PM3 are the same as the PM2, so the forward solution analysis of the kinematic position is the same. For details, see Eqs. (8) to (11).

Here, the coordinate values of S_1, S_2, and S_3 are obtained. Therefore, according to Eq. (12), it is easy to determine the posture parameters of the moving platform of the PM3.

Obviously, from the above analysis process, it is easy to know that the coordinate values of points S_2 and S_3 on the moving platform of the PM3 can be solved by the hybrid branch chain in which they are located. Therefore, taking any point in S_2 and S_3 as the base point, the PM3 has partial motion decoupling.

3.2.2 Inverse position analysis of the PM3

It is easy to know from the topological analysis that the link 6 in hybrid branch chain 1 is perpendicular to the link 5, as shown in Fig. 4(b). Therefore, in the triangles $S_1A_{14}A_{13}$ and $S_1A_{14}A_{12}$, we have

$$S_1A_{13} = \sqrt{l_{16}^2 + l_{15}^2} = l_{17}, \quad S_1A_{12} = \sqrt{l_{16}^2 + (l_{12} + l_{15})^2} = l_{18}.$$

According to the link length equation by constraint $S_1A_{12} = l_{18}$, it is easy to know

$$\theta_1 = 2 \arctan \left(\frac{n_1 + N\sqrt{n_1^2 + n_2^2 - n_3^2}}{n_2 + n_3} \right) (N = \pm 1) \tag{22}$$

Where: $n_1 = -2l_{11}y_{s1}$, $n_2 = -2l_{11}(a + l_{10}/2 - z_{s1})$, $n_3 = l_{18}^2 - l_{11}^2 - (a - x_{s1})^2 - y_{s1}^2 - (a + l_{10}/2 - z_{s1})^2$.

According to the link length equation by constraint $S_1A_{13} = l_{17}$, we have

$$\alpha_1 = 2 \arctan \left(\frac{m_1 + M\sqrt{m_1^2 + m_2^2 - m_3^2}}{m_2 + m_3} \right) (M = \pm 1) \tag{23}$$

Where: $m_1 = 2l_{12}(l_{11} \sin \theta_1 - y_{s1})$, $m_2 = -2l_{12}(a + l_{10}/2 - l_{11} \cos \theta_1 - z_{s1})$, $m_3 = l_{17}^2 - l_{18}^2 - l_{12}^2$.

According to the link length equation by constraint $A_{13}A_{22} = l_{14}$, it is easy to know

$$\theta_2 = 2 \arctan \left(\frac{q_1 + Q\sqrt{q_1^2 + q_2^2 - q_3^2}}{q_2 + q_3} \right) (Q = \pm 1) \tag{24}$$

Where: $q_1 = -2l_{13}(l_{11} \sin \theta_1 + l_{12} \sin \alpha_1)$, $q_2 = 2l_{13}(-l_{10} + l_{11} \cos \theta_1 + l_{12} \cos \alpha_1)$,
$q_3 = l_{14}^2 - l_{13}^2 - (l_{11} \sin \theta_1 + l_{12} \sin \alpha_1)^2 - (-l_{10} + l_{11} \cos \theta_1 + l_{12} \cos \alpha_1)^2$.

Because the hybrid branched chains 2 and 3 in PM3 are the same as PM2, the inverse solution analysis of their positions is the same. For details, see Eqs. (15) to (18).

3.3. Forward position analysis of the PM4

The coordinate system established for PM4 is similar to the PM3, as shown in Fig. 5(a). The hybrid branch chain 1 parameters are labeled as shown in Fig 5(b), and the link length parameters are as follows: $A_{11}A_{12} = A_{11}A_{21} = l_{10}$, $A_{12}A_{13} = l_{11}$, $A_{13}S_1 = l_{12}$, $A_{21}A_{22} = l_{13}$, $A_{22}S_1 = l_{14}$, $A_{13}A_{22} = l_{15}$.

3.3.1. Forward position analysis of the PM4

For forward solution analysis of hybrid branch chain 1, the line $A_{13}S_1$ is perpendicular to the line $A_{22}S_1$ in hybrid branch chain 1, and the angle between the line $A_{13}S_1$ and $A_{13}A_{22}$ is $\gamma_1 = 30°$.
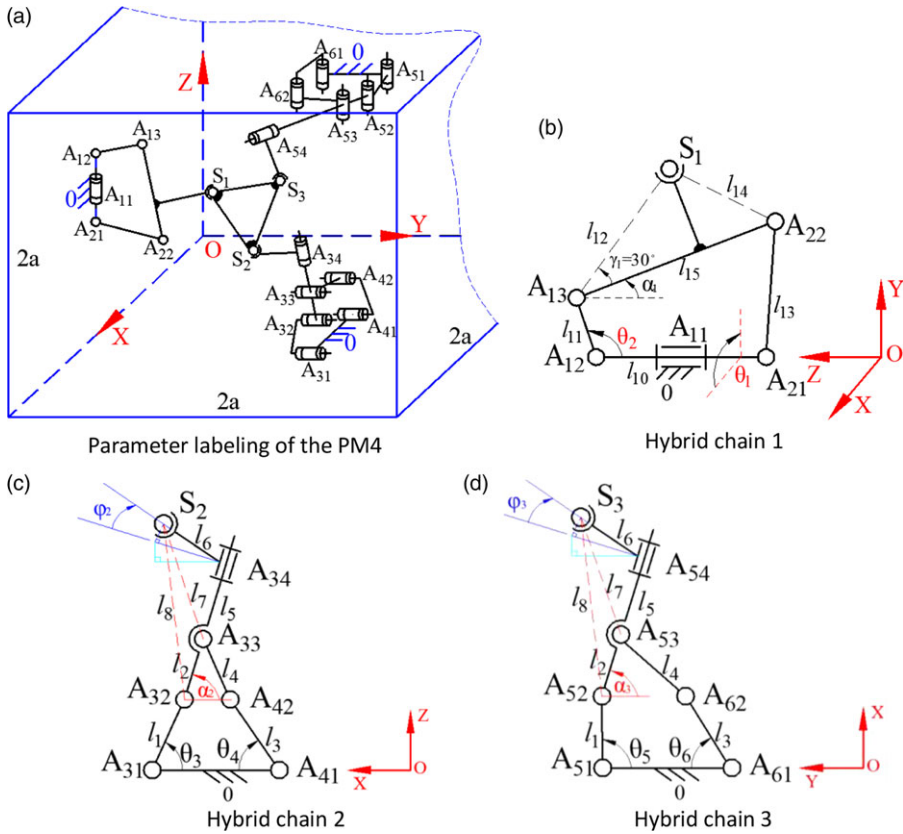
Figure 5. *Kinematic parameter labeling of the parallel mechanism 4.*

Also assign the angle between the link $A_{13}A_{22}$ and the negative direction of Z-axis as α_1, which is taken as the intermediate variable. It's easy to know the coordinates of the following points.

$A_{11} = (a, 0, a), A_{21} = (a, 0, a - l_{10}), A_{12} = (a, 0, a + l_{10}), A_{13} = (a + l_{11} \sin\theta_2 \cos\theta_1, l_1 \sin\theta_2 \sin\theta_1, a + l_{10} - l_{11} \cos\theta_2),$

$A_{22} = (a + (l_{11} \sin\theta_2 + l_{15} \sin\alpha_1) \cos\theta_1, (l_{11} \sin\theta_2 + l_{15} \sin\alpha_1) \sin\theta_1, a + l_{10} - l_{11} \cos\theta_2 - l_{15} \cos\alpha_1).$

According to the link length equation by constraint $A_{21}A_{22} = l_3$, the intermediate variable α_1 is given by

$$\alpha_1 = 2 \arctan\left(\frac{N_1 + n\sqrt{N_1^2 + N_2^2 - N_3^2}}{N_2 + N_3}\right) (n = \pm 1) \tag{25}$$

Where: $N_1 = 2l_{11}l_{15} \sin\theta_2$, $N_2 = -2l_{15}(2l_{10} - l_{11} \cos\theta_2)$, $N_3 = l_{13}^2 - l_{15}^2 - (l_{11} \sin\theta_2)^2$ $-(2l_{10} - l_{11} \cos\theta_2)^2$.

Then we have

$$S_1 = (a + (l_{11} \sin\theta_2 + l_{12} \sin(\gamma_1 + \alpha_1)) \cos\theta_1, (l_{11} \sin\theta_2 + l_{12} \sin(\gamma_1 + \alpha_1)) \sin\theta_1, a + l_{10} - l_{11} \cos\theta_2$$
$$-l_{12} \cos(\gamma_1 + \alpha_1))$$

The hybrid branch chains 2 and 3 in the PM4 are the same as the PM1. Therefore, their forward position solution analysis is the same. For details, please refer to Eqs. (10)-(13) in Ref. [29].

Among them, the angle φ_2 and φ_3 set in the hybrid branch chain 2 and 3 can be obtained successively by the link length constraint $S_1S_2 = \sqrt{3}b$ and $S_1S_3 = \sqrt{3}b$, respectively

$$\varphi_2 = 2 \arctan \left(\frac{H_1 + h\sqrt{H_1^2 + H_2^2 - H_3^2}}{H_2 + H_3} \right) (h = \pm 1) \tag{26}$$

Where, $H_1 = 2l_6(y_{s1} - y_{A34})$, $H_2 = -2l_6(x_{s1} - x_{A34}) \sin \alpha_2 - 2l_6(z_{s1} - z_{A34}) \cos \alpha_2$, $H_3 = 3b^2 - l_6^2 - (x_{s1} - x_{A34})^2 - (y_{s1} - y_{A34})^2 - (z_{s1} - z_{A34})^2$.

$$\varphi_3 = 2 \arctan \left(\frac{G_1 + g\sqrt{G_1^2 + G_2^2 - G_3^2}}{G_2 + G_3} \right) (g = \pm 1) \tag{27}$$

Where, $G_1 = 2l_6(z_{s1} - z_{A54})$, $G_2 = -2l_6(x_{s1} - x_{A54}) \cos \alpha_3 - 2l_6(y_{s1} - y_{A54}) \sin \alpha_3$, $G_3 = 3b^2 - l_6^2 - (x_{s1} - x_{A54})^2 - (y_{s1} - y_{A54})^2 - (z_{s1} - z_{A54})^2$.

By substituting the coordinate values of S_1, S_2, and S_3 into Eq. (12), the posture parameters of the moving platform of the PM4 can be solved.

Through the position analysis of the PM4, it can be easily known that the coordinate values of point S_1 on its moving platform can be obtained by solving the hybrid chain 1 to which it belongs. Therefore, when taking S_1 as the base point, PM4 has the characteristic of partial motion decoupling.

3.3.2 Analysis of inverse position solution of the PM4

For analysis of the inverse solution of the position of the hybrid branch chain 1.

From the forward solution analysis, it is easy to know that S_1 coordinates are given below.

$$\begin{cases} x_{s1} = a + (l_{11} \sin \theta_2 + l_{12} \sin (\gamma_1 + \alpha_1)) \cos \theta_1 \\ y_{s1} = (l_{11} \sin \theta_2 + l_{12} \sin (\gamma_1 + \alpha_1)) \sin \theta_1 \\ z_{s1} = a + l_{10} - l_{11} \cos \theta_2 - l_{12} \cos (\gamma_1 + \alpha_1) \end{cases} \tag{28}$$

From Eq. (36), we have

$$\theta_1 = \arctan \left(\frac{y_{s1}}{x_{s1} - a} \right) \tag{29}$$

$$\theta_2 = 2 \arctan \left(\frac{f_1 + F\sqrt{f_1^2 + f_2^2 - f_3^2}}{f_2 + f_3} \right) (F = \pm 1) \tag{30}$$

where: $f_1 = \frac{-2l_{11}y_{s1}}{\sin \theta_1}$, $f_2 = 2l_{11}(z_{s1} - a - l_{10})$, $f_3 = l_{12}^2 - l_{11}^2 - (y_{s1}/\sin \theta_1)^2 - (z_{s1} - a + l_{10})^2$.

The hybrid branch chains 2 and 3 in the PM4 are the same as the PM3. Therefore, their inverse position solution analysis is the same. See Eqs. (19)–(24) for details in Ref. [29].

3.4. Deterministic analysis of MD and SFP for a three-chain 6-DOF PMs

According to Ref. [29], it is known that the 3A model discussed in this paper does not have SFP solutions.

From the analysis of Section 2.1.1, Section 2.2.1, and Section 2.3.1 above, it is found that all the PM2, PM3, and PM4 (i.e., 3C, 1A + 2C, 2A + 1C) have SFP solutions and MD. The reasons can be revealed and concluded below.

All positions of the 5-DOF branch chain C contained in these three mechanisms can be solved by the constraints of the branch chain itself, that is, the position of the branch chain C is completely deterministic.

It also means that when the center of spherical joint S at the end of the PM is taken as the base point, the PM has the character of partial MD. Therefore, for a general three-branch 6-DOF PM, if one of its hybrid branches has position determinism, the PM has partial MD and SFP performance.

Table II. *Forward position solution for parallel mechanism 2.*

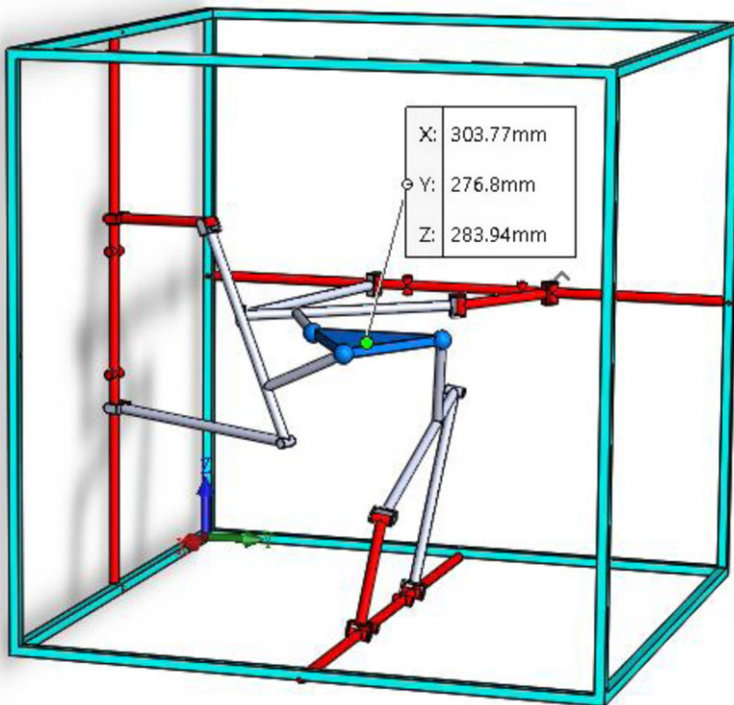|	x/mm	y/mm	z/mm	α/rad	β/rad	γ/rad
1	276.4340	149.7005	170.2476	−0.5150	1.4079	−0.8250
2	270.9279	168.2787	284.7002	−1.2233	1.3910	0.0004
3	309.2812	258.2219	169.4936	1.0058	0.3516	−0.1272
4*	303.7751	276.8002	283.9462	0	0	0

Figure 6. *Three-dimensional computer-aided design model of parallel mechanism 2.*

4. Numerical examples of position analysis

4.1. An example of position analysis of the PM2

4.1.1 Forward position solution

Let the dimensional parameters of the PM2 be (unit: mm):

$a = 300, l_0 = 100, l_1 = l_4 = 120, l_2 = 120\sqrt{3}, l_3 = 220, l_5 = 240, h = 60\sqrt{3}$.

According to the dimensional parameters, a three-dimensional (3-D) computer-aided design (CAD) model of the PM2 was established, and from which the initial input angles (unit: rad) of the six actuated joints $R_i(i = 1 \sim 6)$, namely $\theta_1 = 1.2769, \theta_2 = 1.6087, \theta_3 = 1.4099, \theta_4 = 1.4488, \theta_5 = 1.6315, \theta_6 = 0.8430$ as well as the corresponding output values of the moving platform center point O', namely $x = 303.77, y = 276.80, z = 283.94, \alpha = 0, \beta = 0, \gamma = 0$, are measured. The 3-D CAD model of PM2 is shown in Fig. 6.

By substituting the initial input angles $\theta_i(i = 1 \sim 6)$ (unit: rad) of the six actuated joints obtained from the measured 3-D CAD model into the coordinates of each point and solving for φ_2 and φ_3, the coordinate values of S_1, S_2, and S_3 can be determined. Through the forward equation Eq. (12), the output value of the moving platform center O' point can be obtained. The PM2 has eight groups of forward solutions, four of which are real solutions, as shown in Table II.

Table III. *Inverse position solution of the parallel mechanism 2.*

Hybrid branch chains						
			Inverse solution/(rad)			
Hybrid branch chain 1	θ_1	1.2769	θ_2	1		0.7697
				2*		1.6086
Hybrid branch chain 2	θ_3	1.4099	θ_4	1		0.8082
				2*		1.4488
Hybrid branch chain 3	θ_5	1.6316	θ_6	1*		0.8427
				2		1.0386

Table IV. *Forward position solution for parallel mechanism 3.*

	x/mm	y/mm	z/mm	α/rad	β/rad	γ/rad
1	179.6915	288.5342	290.6154	0.0000–0.1592i	0.0000 + 1.9871i	−0.8046
2	115.2887	276.7235	281.3321	0.0000–0.2606i	0.0000 + 1.7068i	−1.2244
3*	303.3581	274.2836	283.0300	0	0	0
4	238.9553	262.4729	273.7467	−0.3780	2.1889	0

The relative error values of the calculated theoretical values compared to the measured values of the positional parameters from the fourth group of forward position solutions, as given by Eq. (6) with n = −1, Eq. (8) with m = −1, and Eq. (10) with q = −1, are all within 0.1%. Therefore, the derivation of the symbolic forward position solution formulas is correct. Here, we calculate the relative error by taking the difference between the theoretical calculated values and the measured values and then dividing it by the measured values. The measured values can be obtained by using the ruler tool in SolidWorks software to directly measure the virtual simulation model.

4.1.2 The inverse solution example of the PM2
The output values of the center of the moving platform point O' measured in the 3-D model of the PM2 are $x = 303.77, y = 276.80, z = 283.94, \alpha = 0, \beta = 0, \gamma = 0$, respectively, and which are substituted into the inverse solution Eqs. (13)–(18) to obtain the inverse solution input values corresponding to each branch chain, as shown in Table III.

According to Table III, the relative error values of inverse solution and 3-D model measurement in each hybrid branch chain are within 0.01%, indicating that the derivation of the position inverse solution formula is correct.

4.2. An example of kinematic position analysis of the PM3
4.2.1 Example of forward position solution for the PM3
Let the dimension parameter of hybrid branch chain 1 in PM3 be (unit: mm): $a = 300, l_{10} = 130, l_{11} = l_{13} = 100, l_{12} = l_{14} = 120, l_{15} = 150, l_{16} = 110$. The size parameters of other members are the same as PM2.

According to these dimensional parameters, a 3-D model of the PM3 is established, and from which six initial input angles (unit: rad) of the actuated joints $R_i(i = 1 \sim 6)$ are measured, namely $\theta_1 = 2.6060, \theta_2 = 1.5273, \theta_3 = 1.4146, \theta_4 = 1.4354, \theta_5 = 1.6321, \theta_6 = 0.8126$. The corresponding output values of the moving platform center O' are $x = 302.14, y = 275.41, z = 283.92, \alpha = 0, \beta = 0, \gamma = 0$, respectively.

By inputting the initial input angles $\theta_i(i = 1 \sim 6)$ (unit: rad) of the six actuated joints measured from the 3-D model into the coordinates of each point, the coordinate values of S_1, S_2, and S_3 can be easily obtained by solving $\alpha_i(i = 1, 2, 3)$ and φ_1. Using the position forward kinematics Eq. (12), the output value of the center O' of the moving platform can be obtained. There are 16 groups of forward equations for the PM3, but only four groups of which have real solutions, as shown in Table IV.

Table V. *Inverse position solution of the parallel mechanism 3.*

Hybrid branch chains		Inverse solution/(rad)		Intermediate variables/(rad)			Inverse solution/(rad)	
Hybrid branch chain 1	θ_1	1	−0.0470	α_1	1	1.3736	θ_2	1	0.3224
								2	2.7028
					2	1.9027		3	−0.0730
								4	2.0811
		2*	2.6140		3	0.6643		5	0.0639
								6*	1.5265
					4	1.1935		7	0.7546-0.4182i
								8	0.7546 + 0.4182i
Hybrid branch chain 2	θ_3	1			1.4181		θ_4	1	0.8090
								2*	1.4377
Hybrid branch chain 3	θ_5	1			1.6321		θ_6	1	0.8397
								2*	1.0251

The third group of position-real solutions corresponds to the values of the position parameter measured by the 3-D model, and the relative error value is less than 0.1%, which shows that the symbolic positional forward solution formulas are correctly derived.

4.2.2 Example of inverse position solution of the PM3

The output values of the center of the moving platform point O' measured in the 3-D model of the PM3 are $x = 302.14, y = 275.41, z = 283.92, \alpha = 0, \beta = 0, \gamma = 0$, respectively, and are substituted into the inverse solution formula in Section 3.2.2. Inverse solution input values corresponding to each branch chain are obtained, as shown in Table V.

According to Table V, we found that the relative errors of the theoretical calculated values of inverse solution marker (*) and the measured values of the 3D model are both within 0.01%, so the symbolic position inverse solution formula is correctly derived.

4.3. An example of kinematic position analysis of the PM4

4.3.1 Example of forward position solution for the PM4

The parameters of the hybrid branch chains 2 and 3 in the PM4 are set to be the same as those in the PM1, while the parameters of the hybrid branch chain 1 are specified as follows (unit: mm):

$$l_{10} = 100, l_{11} = l_{14} = 120, l_{12} = 120\sqrt{3}, l_{13} = 220, l_{15} = 240.$$

According to the corresponding dimensional parameters, a 3-D CAD model of the PM4 is established, and the initial input angles (unit: rad) of the six actuated joints $R_i (i = 1 \sim 6)$ are measured from it, namely $\theta_1 = 1.3626, \theta_2 = 1.2748, \theta_3 = 2.6182, \theta_4 = 1.7171, \theta_5 = 2.3880$, and $\theta_6 = 1.1126$. The respective output values of the moving platform center O' point are $x = 278.61, y = 277.31, z = 243.53, \alpha = 0, \beta = 0, \gamma = 0$.

According to the verification process of the PM1, the output value of the center point O' of the moving platform is obtained through the position forward kinematics Eq. (12). There are 32 groups of position forward kinematics equations for the PM4, but only 2 groups of which have real solutions, as shown in Table VI.

The second group of positional real forward solutions corresponds to $n = -1$ in Eq. (25), $h = -1$ in Eq. (26), $g = -1$ in Eq. (27), and the positional parameter values measured by the 3-D model, and their

Table VI. *Forward position solution for the parallel mechanism 4.*

	x/mm	y/mm	z/mm	α/rad	β/rad	γ/rad
1	314.8944	330.6946	278.2279	0.9407	0.2956	0.9631
2*	278.6097	277.3345	243.5465	0.0000	0.0214	−0.0002

Table VII. *Inverse position solution of the parallel mechanism 4.*

Hybrid branch chains		Inverse solution/(rad)		Intermediate variables/(rad)		Inverse solution/(rad)		
Hybrid branch chain 1	θ_1	1	1.3625	\		θ_2	1	0.8579
							2*	1.2749
Hybrid branch chain 2	θ_3	1	−0.4340	1	1.0930	θ_4	1	0.2428
							2	−2.9009
							3	−0.4423
				2	1.8001		4	2.1298
							5	−0.2502
				3	0.3840		6*	1.7171
		2*	2.6182				7	0.7703 − 0.2247i
				4	1.0911		8	0.7703 + 0.2247i
Hybrid branch chain 3	θ_5	1	−0.4101	1	1.0043	θ_6	1	0.4060
							2	−2.7431
				2	1.6769		3	−0.3293
							4	2.3295
		2*	2.3879	3	0.3009		5	−0.1561
							6	1.8897
				4	0.9736		7	0.6698
							8*	1.1128

relative error values are all within 0.1%. Therefore, the symbolic positional forward solution formula is derived correctly.

4.3.2 Example of inverse position solution of the PM4
The measured output value of the center *O'* point of the moving platform in the 3-D model of the PM4 is substituted into the inverse solution Eqs. (28)–(30) in this paper and Eqs. (19)–(24) in Ref. [29] to obtain the inverse input value corresponding to each branch chain, as shown in Table VII.

As can be seen from Table VII, the relative error values of the theoretical values of the PM4 and the measured values of the 3-D model are within 0.01%, which shows the symbolic position inverse solution formula is correctly derived.

5. Workspace analysis

In order to understand the workspace characteristics of different topologies, PM1 and PM2 are selected for workspace analysis.

5.1. Position workspace

The positional workspace mentioned in this paper refers to the set of points that can be reached by the center of the moving platform when the posture angles of the end moving platform of the mechanism are all zero degrees ($\alpha = 0, \beta = 0, \gamma = 0$).
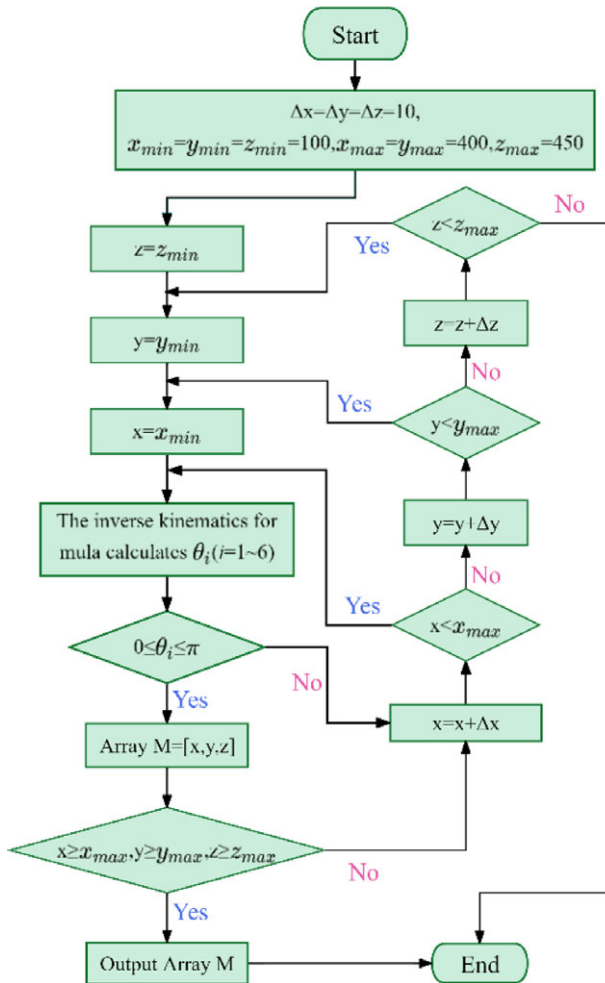
Figure 7. *Flow chart of calculating the position workspace of the parallel mechanism.*

This paper uses the numerical discrete search method based on the inverse solution of kinematics to calculate the position workspace of the PM, that is, according to the structural parameters of the PM1 and PM2 and the three-dimensional model established by SolidWorks software, the posture angle of the mechanism is set as $\alpha = 0, \beta = 0, \gamma = 0$, and the workspace range of the PM1 and PM2 is estimated as $x \in [100, 400], y \in [100, 400], z \in [100, 450]$. Then, the angles of PM1 and PM2 actuated joints are calculated, respectively, by using the formula (16–24) in Ref. [29] and the inverse kinematics solution formula (13–18) in this paper to check whether the angles of PM1 and PM2 meet the set range of actuated joints ($\theta_i \in [0, \pi](i = 1, 2, 3, 4, 5, 6)$). The specific calculation process is shown in Fig. 7.

When $\alpha = 0, \beta = 0, \gamma = 0$, the position workspace of PM1 and PM2 is shown in Fig. 8 and Fig. 9.

5.2. Posture workspace

The posture workspace is a collection of points in the space where the moving platform at the end of the PM is fixed. Firstly, the fixed position of the moving platform was set as $x = 250, y = 250, z = 250$, and the spatial range of the posture angle of the PM was estimated as $\alpha \in [-\pi/2, \pi/2], \beta \in [-\pi/2, \pi/2], \gamma \in [-\pi/2, \pi/2]$. Then, the inverse position solution formula of PM1 and PM2 is used to calculate the angle of the actuated joint and determine whether it is within the set angle range of the
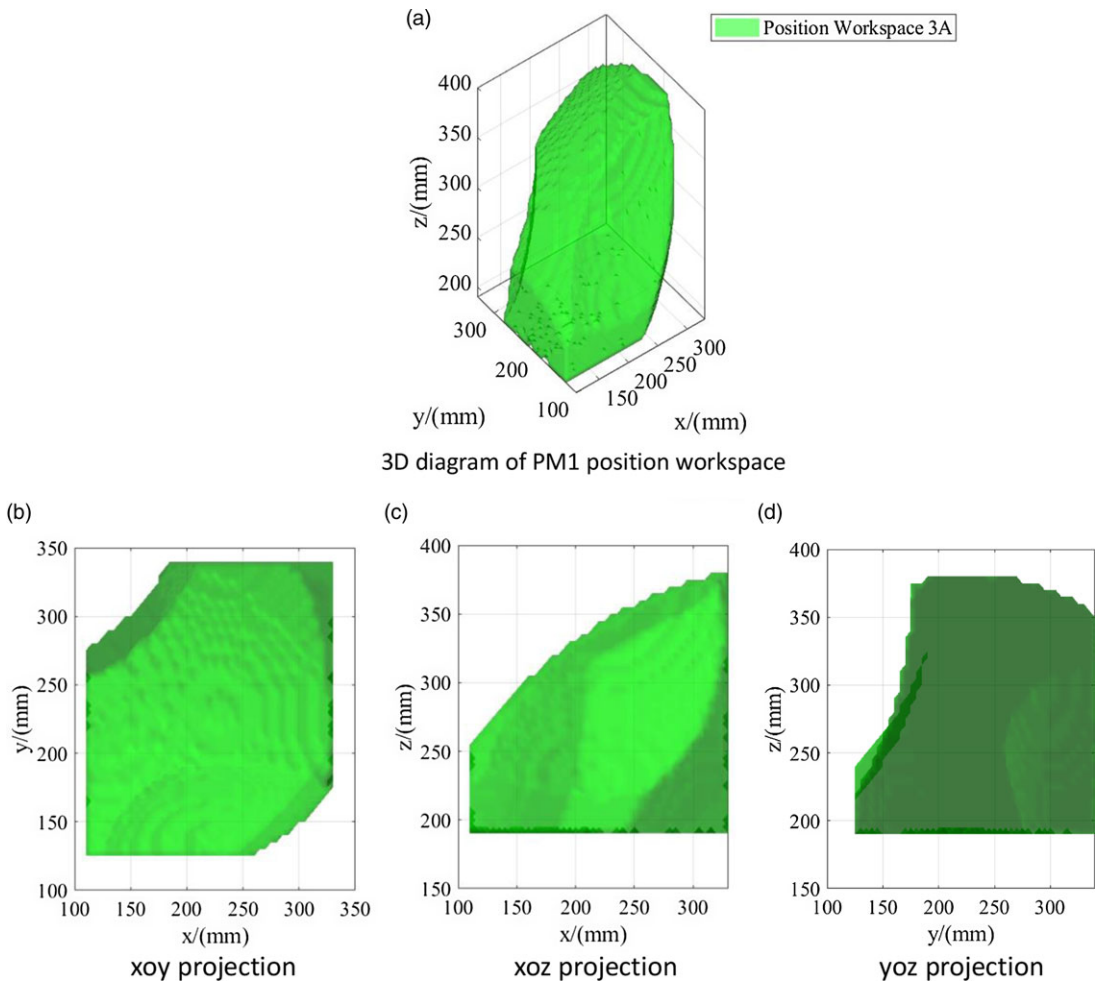
Figure 8. *Position workspace for parallel mechanism1 ($\alpha = 0, \beta = 0, \gamma = 0$).*

actuated joint ($\theta_i \in [0, \pi](i = 1, 2, 3, 4, 5, 6)$). The calculation process of the posture workspace is similar to that of the position workspace, as shown in Fig. 7.

When $x = 250, y = 250, z = 250$, the posture workspace of PM1 and PM2 is shown in Fig. 10.

Based on Figs. 8–10 above, we find that

When the posture angles are the same ($\alpha = 0, \beta = 0, \gamma = 0$), the position workspace of PM1 is much larger than that of PM2.

In the same position state ($x = 250, y = 250, z = 250$), the posture workspace of PM1 is also larger than that of PM2.

6. Conclusions

Based on the designed 6-DOF branch chain A and 5-DOF branch chain C, three 6-DOF parallel mechanisms with motion decoupling and symbolic forward position solutions are proposed in this paper, the symbolic forward and inverse position formulas of three of which are derived and verified by numerical examples.

It is found from this work that if the position or orientation of a point on the moving platform can be determined by the determination of the known positions of the hybrid branch chains, then the PM has
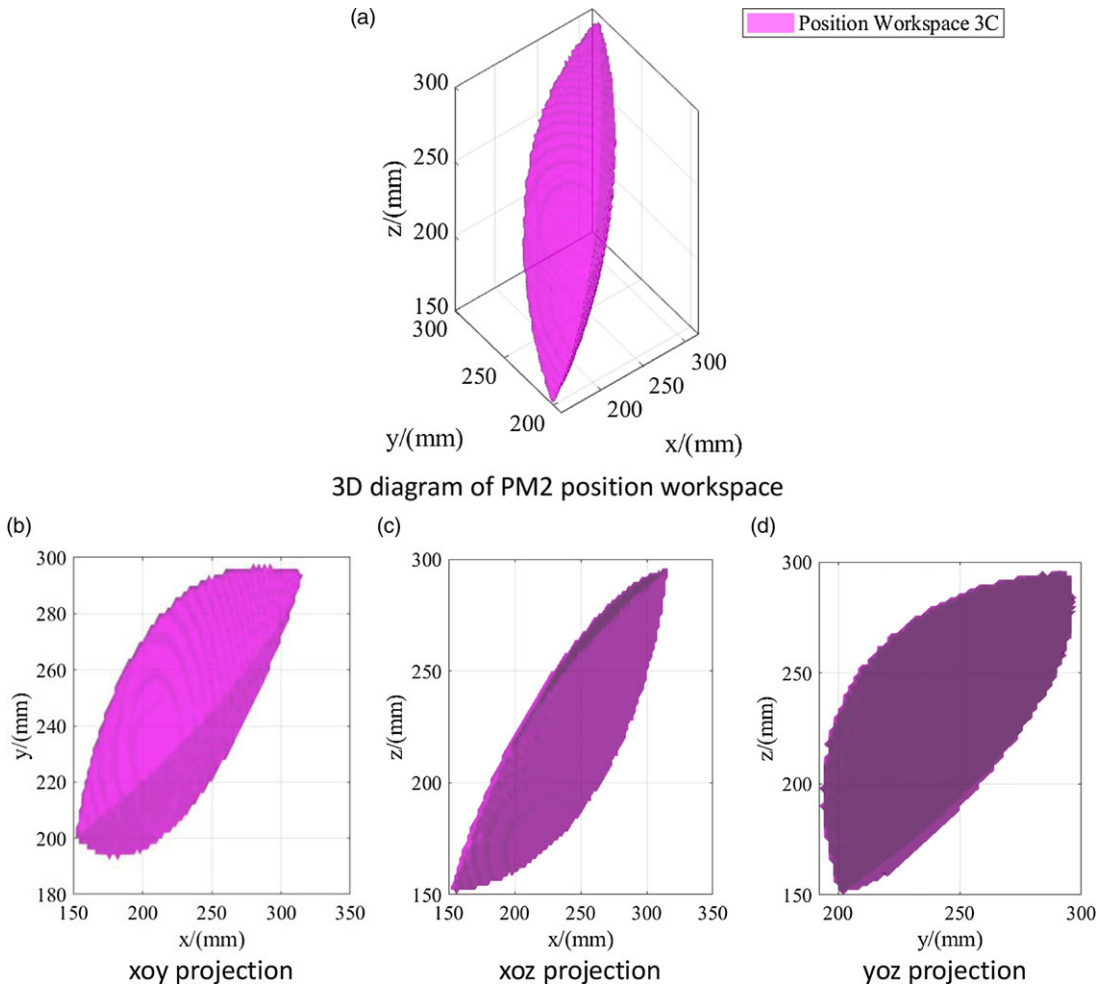
Figure 9. *Position workspace for parallel mechanism 2 ($\alpha = 0$, $\beta = 0$, $\gamma = 0$).*
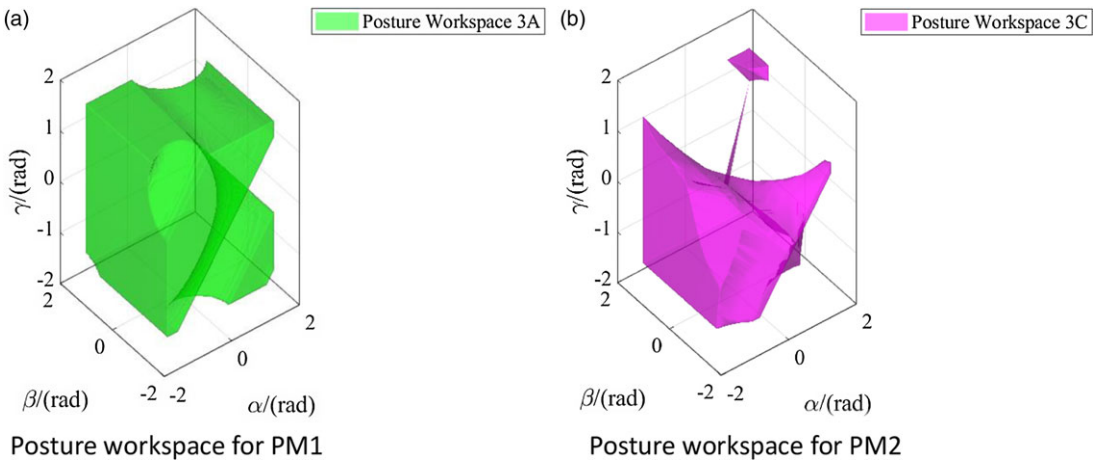

Figure 10. *Posture workspace ($x = 250$, $y = 250$, $z = 250$).*

partial motion decoupling and symbolic forward position solutions. Therefore, all 6-DOF PMs containing the 5-DOF branch chain C (PMs 2, 3, and 4) have the characteristics of partial motion decoupling and symbolic forward position solutions, which is the contribution of the work.

This paper provides a new insight into the design and position analysis of 6-DOF PMs with symbolical forward and inverse kinematics solutions, as well as partial motion decoupling.

References

[1] Z. H. Guo, Q. Q. Du and Q. Z. Yang, "Forward and inverse position kinematics analysis of a new 3-PRRS parallel mechanism," *China Mech Eng* **26**(4), 451–455,463 (2015).

[2] T. Z. Yu and H. P. Shen, "An Easily Manufactured Structure and Its Analytic Solutions for Forward and Inverse Position of 1-2-3-SPS Type 6-DOF Basic Parallel Mechanism," 2012," **In:** *IEEE International Conference on Robotics and Biomimetics (ROBIO 2012)*, Guangzhou, China (2012).

[3] H. P. Shen, *Topological Characteristics-Based Kinematics for Robotic Mechanism* (Higher Education Press, Beijing, (2021).

[4] H. P. Shen, Y. Tang, G. L. Wu and J. Li, "Design and Analysis of a Class of Two-Limb Non-Parasitic 2T1R Parallel Mechanism with Decoupled Motion and Symbolic Forward Position Solution -influence of Optimal Arrangement of Limbs Onto the Kinematics, Dynamics and Stiffnes, "*Mech Mach Theory* **172**, 104815 (2022).

[5] C. Innocenti and V. Parenti-Castelli, "Closed-form direct position analysis of a 5-5 parallel mechanism," *J Mech Design* **115**(3), 515–521 (1993).

[6] W. Lin, C. D. Crane and J. Duffy, "Closed-Form Forward Displacement Analysis of the 4-5 in-Parallel Platform," **In:** *Proceedings of the 22nd Biennial Mechanisms Conference*, Scottsdale, AZ, USA. Scottsdale (ASME, 1992) pp. 521–527.

[7] X. G. Huang, L. L. Li, Q. Z. Liao and D. L. Li, "Direct Kinematics for a general 6-5 Planar parallel mechanism," **In:** *Proceedings of the 10th International Conference on Applications of Mechanism and Machine Science in China (2013 CCAMMS)*, (2013). pp. 131–133.

[8] L. Han, F. Wen and C. G. Liang, "Forward displacement analysis of the 6-5 stewart platform," *J Beijing Univ Posts Telecom* **21**(2), 33–42 (1998).

[9] Y. Zhang, Q. Z. Liao and S. M. Wei, "Forward displacement analysis of a general 6-4 in-parallel platform," *J Mech Eng* **48**(9), 26–32 (2012).

[10] N. Su, Q. Z. Liao and S. G. Liang, "Forward positional analysis for a kind of 5-5Platform in-parallel robotic mechanism," *J Beijing Univ Posts Telecomm* **03**, 4–11 (1997).

[11] H. L. Yun, F. Gao and B. Wang, "Position analysis on parallel mechanism with 3 branch chains and 6-DOF," *J Mech Design* **07**, 57–60 (2006).

[12] Z. Gao and F. Gao, "Kinematics analysis of a new 6-DOF parallel mechanism," *Mach Design Res* **05**, 45–48 (2006).

[13] Z. Gao, F. Gao and R. Su, "Forward position analysis of a 6-DOF 3-urPS parallel mechanism," *China Mech Eng* **07**, 846–850 (2007).

[14] Q. K. Yu, Y. P. You and J. Y. Han, "Position analysis of 3-urSR parallel mechanism with 6-DOF," *Trans Chinese Society Agri Mach* **42**(12), 215–219 (2011).

[15] C. Innocenti and V. Parenti-castelli, "Forward Kinematics of the General 6-6 Stewart Fully-Parallel Mechanism: An Exhaustive Numerical Approach via a Mono- Dimensional-Search Algorithm," **In:** *Proceedings of the 22nd Biennial Mechanisms Conference*, Scottsdale, AZ, USA. scottsdale (ASME, 1992) pp. 13–16.

[16] B. Dasgupta and T. S. Mruthyunjay, "A constructive predictor-corrector algorithm for the direct position kinematics problem for a general 6-6 stewart platform," *Mech Mach Theory* **31**(6), 799–811 (1996).

[17] M. L. Husty, "Algorithm for solving the direct kinematic of stewart-gough-type platforms," *Mech Mach Theory* **31**(4), 365–380 (1996).

[18] C. W. Wampler, "Forward displacement analysis of general six-in-parallel sps (Stewart) platform manipulator using soma coordinates," *Mech Mach Theory* **31**(3), 311–337 (1996).

[19] P. Nanua and K. J. Waldron, "Direct Kinematic Solution of a Stewart Platform," **In:** *Proceedings of the IEEE International Conference on Robotics and Automation -1989*, Columbus, OH, USA. piscataway (Ohio State Univ, IEEE, 1989) pp. 431–437.

[20] W. Lin, J. Duffy and M. Griffs, "Forward Displacement Analyses of the 4-4 Stewart Platforms," **In:** *Proceedings of the 21st Biennial Mechanism Conference. September 16-19*, Gainesville, United States. New York (Univ. of Florida, ASME, 1990) pp. 263–269.

[21] L. L. He and H. Z. Liu, "A solution for forward kinematics of 6-DOF parallel platform based on genetic algorithm and neural network," *Mech Sci Tech* **11**, 1348–13511355 (2004).

[22] L. L. He and H. Z. Liu, "Research on forward solution of position of 6-DOF hybrid driven parallel mechanism," *China Mech Eng* **08**, 920–923970 (2007).

[23] J. B. Zhao, F. Gao and Y. Yue, "Forward and inverse displacement analysis of 6-PPPS orthogonal 6-DOF parallel mechanism," *Mech Sci Tech* **01**, 96–101 (2008).

[24] H. P. Shen, T. L. Yang and C. H. Ma, "A class of 6-DOF parallel kinematic structures and structure analysis," *China Mech Eng* **06**, 721–724 (2008).

[25] H. P. Shen, H. B. Yin, Z. Wang, T. Huang, J. Li, J. M. Deng and T. L. Yang, "Research on forward position solutions for 6-SPS parallel mechanisms based on topology structure analysis," *J Mech Eng* **49**(21), 70–80 (2013).

[26] Q. M. Wang, J. Su, Y. R. Zhang, Z. C. Lu, H. Y. Lin and G. Xu, "Structure characteristics and kinematic analysis of redundant 6-DOF parallel mechanism," *J Mech Eng* **53**(18), 121–130 (2017).

[27] Y. H. Chen, T. S. Zhao, M. C. Geng, F. H. Yuan and E. W. Li, "Kinematic analysis of a 6-DOF parallel mechanism with closed loop dual-drive and composite output," *China Mech Eng* **26**(20), 2793–28002805 (2015).

[28] Q. Qu, "Forward kinematics analysis of 6-DOF parallel mechanism based on differential evolution method," *Mach Tools Hydra* **44**(13), 83–88 (2016).

[29] Z. Q. Du, J. Li, H. T. Liu, Y. N. Zhao and H. P. Shen, *Design of a Three-Chain 6-DOF Symmetrical Parallel Mechanism and Solutions of Its Forward and Inverse Kinematics[C]//IFToMM World Congress On Mechanism and Machine Science* (Springer Nature Switzerland, Cham, (2023). pp. 207–217.

[30] T. L. Yang, A. X. Liu and H. P. Shen, *Theory and Application of Robot Mechanism Topology* (Science Press, Beijing, (2012).